**Title: Power flow formulation for LVDC microgrids with nonlinear load models**

**Authors**: Irina Ciornei, Andres Felipe Martinez Palomino, Mihaela Albu and Mihai Sanduleac

Published in: Conference Proceedings of IEEE IDCM, Nurnberg, Germany

DOI (link to publication from Publisher): pending

Publication date: 06/2017

# Power flow formulation for LVDC microgrids with nonlinear load models

Irina Ciornei
Mihaela Albu
Mihai Sanduleac
MicroDERLab, University Politehnica of Bucharest
Bucharest, Romania
e-mail: irina.ciornei@upb.ro, albu@ieee.org, mihai.sanduleac@upb.ro

Andres Felipe Martinez Palomino
Politecnico di Torino
Turin, Italy
e-mail: andresfelipe.martinezpalomino@studenti.polito.it

***Abstract*—Low voltage direct current microgrids are seen as key components of the future smart grids together with their AC counterparts. In the analysis of such microgrids the loads are modelled most of the times as constant power loads (CPL). This paper proposes a quantification of the flexibility introduced by several DC loads, generally available in low voltage DC microgrids as in-use appliances. The analysis is based on a power flow formulation that takes into account the droop control coefficients and that includes the actual non-linear characteristics of such loads. The models we use for the flexible DC loads were experimentally derived through a measurement scenario built on steady-state time intervals of 10s.**

***Index Terms*—DC microgrids, DC power flow in droop controlled networks, low voltage load modelling.**

## I. INTRODUCTION

Within the last decade one may notice that there is an exponential increase in the deployment of distributed power generation (DG) installed at low voltage distribution feeders, with the dominant technology being rooftop installed PVs. Also, in line with this trend, previously shaped concepts such as active distribution grids [1] are more and more present in the research interests of academia and industry. Traditionally, the distribution grids ware designed with a unidirectional power flow in mind (where the flow of both real and reactive power is always from the higher to lower voltage levels).

The changes within the distribution networks due to the integration of DG may have positive as well as negative impacts to both distribution network service providers (DNSPs) and consumers. Among the positive benefits, the strongest argument is the improvement in environmental impact when DGs use renewable energy sources (RES) [2], while voltage profile improvement and line-loss reduction might be positive or negative according to an optimal or random placement of the DGs within the distribution network [2, 3].

Microgrids and decentralized control at low voltage are emerging trends in line with the concept of active distribution grids. They are also cited as necessary or valuable cells in a network that seeks for increasing its resilience and reliability [1]. A microgrid operating at low voltage composes of distributed generation (DGs), energy storage system (ESS) - which might be or not necessary depending on the type of local generaion mix; and loads. Microgrids have the capability to work either as a stand-alone, independent system, or interconnected to the main distribution grid. Microgrids have been proposed operating either with alternative current (AC), direct current (DC) or a mix of the two, forming the so-called hybrid microgrids[4].

AC power grids have been in operation for decades and their components and mechanisms to keep the power system stable are considered mature enough and well understood. As a consequence most of AC microgrids inherited the operation concepts from the main power grid [5]. A core analysis tool to keep an AC power system on a stable steady state operation is the so-called power flow analysis. It is based on a combination of real-time monitoring/measurements of the states of the system, through measurement units located on a number of nodes and calculations for the rest of the nodes in the system that makes the system fully observable at any moment in time [6].

In the case of the DC microgrids, the management of the power flow in the system, several methods have been proposed; these are mainly based on various control strategies such as Master-slave control [7], average current control method [8], and droop control using virtual impedance [9]. The latter is more and more frequently cited as a common practical approach when paralleling the several DC/DC power converters interfacing RES-based generation to the microgrid [10-12]. Among the major advantages of the voltage droop control strategy for DC microgrids one can underline its simplicity, together with the possibility to make the controller autonomous; moreover, it can be realized with no communication.

A practical and comprehensive approach to formulate the power flow under droop scheme is given in [13]. However, the formulation considers only the constant power load models. A more general, theoretical approach is given in [14]. Note however that this paper focuses on the energy management control, the most upper layer of control. Also the objective function considered here is the classical quadratic cost of fuel similar to dispatch algorithms used for large power plants. This assumption might not hold at all in the case of DC microgrids with RES-based generation and storage systems.

The following sections present a background on the droop control methods as second and third level control for both AC and DC microgrids with an emphasis on similarities in formulation. Then, we present how the actual, non-linear and non-constant aggregated load models were developed. They are based on extensive laboratory measurement tests performed on several types commonly used loads for offices and residential buildings. We then formulate a generalization of the simplified power flow model proposed in [15], using the aggregated load models derived in the previous step. Simulated results for the proposed generalized power flow conclude our work.

## II. Background and Preliminaries

### A. Droop control in AC and DC grids

A brief review of the principles of droop control in AC grids will be given below with an emphasis on the analogy of the voltage droop control principles for DC microgrids. One of the major aspects of operating AC grids is given by the requirement that load and generation are to be balanced at all times. This is indeed related to the fact that historically energy could not be stored in large quantities and at reasonable prices such that to make it available when needed. A key feature of the droop control principles in AC grids is the use of a global variable (the synchronous frequency) that could indicate the imbalance between load and generation in any bus of the network. Thus, the control equations for an AC grid could be stated as: the active power injection $P_i$ at source $i$ is controlled to be proportional to the deviation of the frequency ($\Delta f_i$) from its nominal value (e.g. 50 Hz in European power networks), such as in (1).

$$P_i = P_i^* - k_i \cdot \Delta f_i \qquad (1)$$

where $k_i > 0$ is the control gain, also known as *droop coefficient*, $P_i^* \in [P_i^{min},\ P_i^{max}]$ is the nominal injection set-point and $P_i^{min}$, and $P_i^{max}$ are the minimum and maximum operation points of source *i*.

### B. Modeling of sources in DC PF for LV DCMGs

The switching devices that interface the generation units such as PVs with the DC bus in the proposed microgrid model might be seen from the power flow point of view as a controlled voltage source with its associated upper level controller, which implements the droop- algorithm. Thus, for the scope of this analysis only the steady-state characteristics of the DC/DC converters are of much importance, while the current and voltage primary controllers (usually PI controllers) might be ignored due to dynamics decoupling. The mathematical model of the source under droop is then written as [15]:

$$V_{ref}^* = V_0 - R_{D_i} * i_G, \qquad (1)$$

where, $V_{ref}^*$ is the reference voltage for the source, which should be equal to the measured value at the bus. To be noted however, that this equation alone does not guarantee to achieve proportional load sharing, unless non-local (distributed or decentralized) secondary controllers were carefully tuned. The math of this equation tells us that this is due to the absence of a global variable such as the frequency in the case of AC power networks [14].

## III. Derivation of DC Compatible Load Models

As said before, loads are usually modelled as constant power loads CPL, but most of the time this is not an accurate model. Derivation of actual models for the loads to be directly supplied in DC helps us understand the behavior of the DC microgrid under abnormal conditions such as under-voltage (dip) or in the restoration process after a black-out. Our approach is to derive the specific model that best fit the steady-state operation characteristic of each type of load.

Nowadays, most of electronic appliances present in a residential or office building have an internal rectifier AC/DC on the supply side to the grid. A question that might be pose is “can these appliances be supplied directly with AC or DC power without changing their performance?” On the theoretical level it was proven that the answer might be yes [16]. To answer this question deeper, we have developed an experiment to test different appliances called devices under test (DUTs) that might be used as “DC ready devices”. It consists to energy at direct voltage to appliances normally designed to be supplied by AC low voltage plugs (regular power supply sockets in offices/houses) and register the steady-state power consumption level at different supplied voltage levels. The results will be compared with AC standards and a proposal for a standard for DC microgrids. Therefore, it was a practical test without changing anything in the internal-rectifiers. Within the literature we have surveyed on this topic we have found few projects attempting to supply in DC several loads. One of them is “Nushima project” [17], in which the island was supplied by a 360 V DC distribution system. In this case, however, appliances were supplied using several energy conversion with DC after a typical DC/DC converter stage and with AC after an AC/DC inverter stage. Another example comes from National Chung Cheng University of Taiwan [18], where several native DC loads were tested and controlled to understand benefits and barriers of DC microgrid. However, no actual derivation of the load models took place. It is worth mentioning that most of the studies surveyed looked mostly on efficiency aspects when comparing the two forms pf power supply AC or DC for low voltage microgrids, rather than developing actual models for DC compatible loads [19, 20].

### A. DUTs

The DUTs are selected because there are the most common used for people in homes/offices and have internal rectifier. They are the emerging technologies, largely deployed on a wide range of home appliances, therefore, they form a class of probably directly compatible loads with DC microgrids.

For the scope of this analysis, DUTs are divided into two types of loads: lighting loads and non-lighting loads. For the lighting loads besides the power, the illuminance is also an important characteristic to be evaluated during the tests and to be corroborated with the corresponding V-I values.

Table I shows the lighting DUTs (bulbs) with their main characteristics, all of them being designed to operates at 230 V AC and 50 Hz. Table II shows the non-lighting DUTs with the nominal specifications, as they are given on the manufacturer manual. In the table there are DUTs for which two values of power consumption are given. They correspond to the different operating modes of the device: stand-by mode (low power) and normal mode (high power). The desktop has different components that operate at different voltages and for this reason there is more than one voltage levels presented.

TABLE I

| Type Lighting DUTs | Lumen [lm] | Temp [K] | Power [W] |
|---|---|---|---|
| Halogen Philps | 1200 | 2800 | 70 |
| Halogen Start | 450 | 2800 | 42 |
| CFL Philips | 1430 | 2700 | 23 |
| CFL Osram | 1430 | 2700 | 14 |
| LED Philips | 470 | 2700 | 5.5 |
| **Type Not-Lighting DUTs** | **AC input Voltage [V/Hz]** | **DC Voltage[V]** | **Power [W]** |
| Notebook HP Compag | 100-240/50-60 | 19 | 90 |
| Cell-phone charger Nokia 1680c. | 100-240/50-60 | 5 | 0.15 |
| Printer HP laserJet | 220-240/50-60 | - | 60-2[1] |
| Display Acer AL1916C | 100-240/47-63 | 5-15 | 60-2 |
| Desktop Dell optix 330 | 90-260/47-63 | 3.3-5-12 | 280 |

## B. Methodology

All DUTs are connected to the source as it is shown below in Figure 1. For DC source a XANTREX model XFR 600-4 is used. The equipment used to provide voltage and current measurements are Fluke 3000 FC and Fluke 289 respectively.

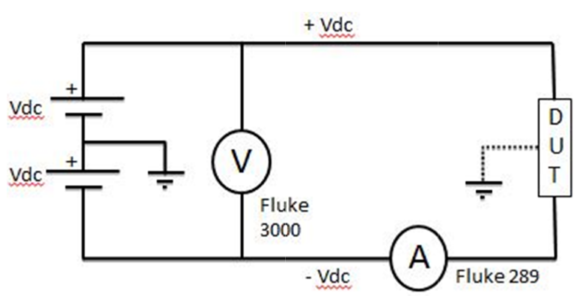


Figure 1. Schematic of DC source connection for DUTs

### 1) Not-Lighting DUTs

After the connection showed in Fig. the DC source starts from 0 V to 400 V, by steps of 10 V. For each step the voltage and current value are recorded in order to draw the experimental I-V characteristic.

After the voltage reaches the level of 400 V, a new stage of the experiments starts. The output voltage starts now at 400 V and finishes at 0 V reducing the voltage level by 10 V in each consecutive step. Again for each step the voltage and current values are recorded for the experimental model of the load. The whole procedure was repeated five times for each procedure: increasing or decreasing the voltage. The final value is the average of the five measurements taken at the specific voltage level when measuring for the specific procedure: increasing/decreasing the voltage. This procedure was followed due to the existence of capacitors in most of the internal power supply of the appliances, which is resulting in a hysteresis-like behavior of the P(U) characteristics.

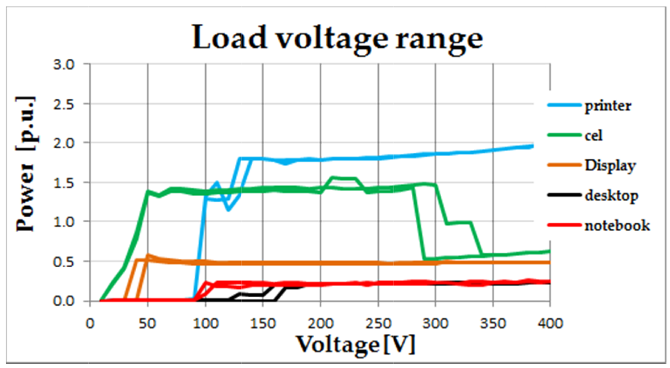


Figure 2. Power characteristics of Not-Lighting DUT

### 2) Lighting DUTs

The lighting DUTs are the bulbs. For these devices also the illuminance was measured. The procedure is the same as for the not-lighting DUTs, but in addition to voltage and current, the iluminance value is also recorded in each step. To measure the illuminance, a luxmeter LT Lutron model LX-1102 was used.

Before starting each measurement session, the illuminance of the room at 0 V was recorded such that to be able to make the difference of the illuminance value at environmental conditions with no artificial lighting system, and with the lighting under measurement on.

## C. Results

The results are presented by graphics with the values on the axis in per unit [p.u.] such that to be able to perform the comparison between DUTs derived models and their corresponding standard characteristic.

### 1) Not-Lighting DUTs

First results are the power characteristics of the not-lighting DUTs shown in Fig. 2. The power is normalized to the AC nominal power of each device. There are three DUTs that consume less power in DC than in AC.

From the data depicted in Figure 2 it is possible to derive the characteristics in Table II. It shows the operation voltage limits for each DUTs such that the device operates with high performance. This is similar to the voltage acceptability curves derived for AC supply [21-23].

From Figure 2 one can see tha the DUTs' curves exhibit three different behaviors depending of the voltage levels: no-operation mode corresponding to zero power consumption. The second is a linear trend in which the DUT is under intermittent operation. Finally, the last curve corresponds to high performance operation and it behaves almost as constant power consumption unit. For each DUT the range of these three operation characteristics is different. Furthermore, there is a little hysteresis for desktop, because the raising of the voltage starts with a 100% performance at 190 V, while when voltage is decreasing, the DUT turns OFF at 160 V.

TABLE II

| **DUTs Not-Lighting** | **Voltage interval for no-operation [V]** | **Voltage range for linear P(V)/ intermittent operation [V]** | **Voltage interval for high Performance [V]** |
|---|---|---|---|
| Notebook | 0-10 | 10 – 110 | 110 – 400 |
| Cell-phone charger | 0-10 | 10-50/ 290-400 | 50 - 290 |
| Printer | 0-90 | 90 - 140 | 140 - 400 |
| Display | 0-30 | 30 - 210 | 210 - 400 |
| Desktop:<br>increasing<br>decreasing | <br>0-180<br>0-20 | <br>-<br>20 - 150 | <br>180 - 400<br>150 - 400 |

The power function model is:

$$P(v) = \begin{cases} 0, \rightarrow v \le V\min \\ Const, \rightarrow V\min \le v \le V\max \end{cases} \quad (2)$$

Vmin and Vmax need to be defined by a standard. Currently there is no official standard for these devices operating directly in DC, besides a German roadmap for developing technical norms [24]. To be noted that the linear and intermittent modes are inside the Vmin value.

TABLE III

| Results Not-Lighting DUTs Voltage Range | | | |
|---|---|---|---|
| **Dispositive /Curve** | **Nominale Voltage AC [V]** | **Min. Voltage [%]** | **Max. Voltage [%]** |
| Notebook | 230 | 47.8 | 173.9 |
| Cell charger | 230 | 21.7 | 130.4 |
| Printer | 230 | 60.9 | 173.9 |
| Display | 230 | 91.3 | 173.9 |
| Desktop | 230 | 78.3 | 173.9 |

| | | | |
|---|---|---|---|
| CBEMA | 120 | 87 | 106 |
| ITIC | 120 | 90 | 110 |
| SEMI | 100 % | 90 | - |
| IEC Class 3 | 230 | 90 | - |
| EMerge A (DC) | 380 | 96 | 110 |

*2) Lighting DUTs*

For the lighting DUTs there are two characteristics when the voltage changes: Power and Illuminance. Fig.3 shows the power characteristics of the lighting DUTs normalized to the nominal power of each DUT. From the Figure 4 one can deduct that at 230 V almost all bulbs are under the 1 p.u. value. It means that their consumption supplied by DC is lower than AC. Also shows the presence of hysteresis for CFL and LED bulbs. For the halogens bulbs the characteristic increasing or decreasing the voltage is the same.

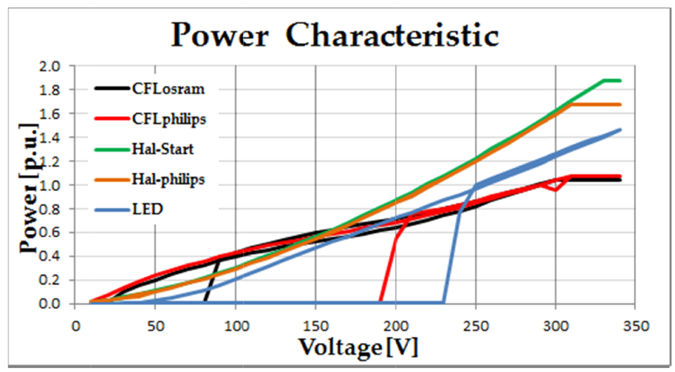

Figure 3. Power Characteristics of Lighting DUTs normalized to nominal power of each bulb

Figure 4 shows the illuminance characteristic of all lighting DUTs normalized to the value measured at 230 V in DC. The characteristics of illuminance are similar to the power. There is presence of hysteresis in CFL and LED bulbs. Because there is no general accepted definition for a high performance of lighting DUT, in this work we define high performance range of operation the range of voltage within 70% to 150%.of the standard 230 V in AC.

From the Figure 5 is deducted that halogen bulbs limit the voltage range for all the lighting DUTs. Table IV shows a comparison between the standards and the voltage range defined by the lighting DUTs.

All lighting DUTs comply the standards. The upper and lower limit is 5 % bigger than the values proposed by Emerge Alliance [23].

The power function model includes the hysteresis behavior, i.e for increasing voltage is defined by (3):

$$P_{CFL}(v) = \begin{cases} 0, \rightarrow v \le V\min \\ A \times v + B, \rightarrow V\min \le v \le V\max \end{cases} \quad (3)$$

While for decreasing voltage is defined by (4):

$$P_{CFL}(v) = A \times v + B \quad (4)$$

where, A and B are constants depending on the appliance type.

The illuminance function model also includes hysteresis behavior; i.e for increasing voltage is defined by (5):

$$L_{CFL}(v) = \begin{cases} 0, \rightarrow v \leq V\min \\ A \times v^2 + B \times v + C, \rightarrow V\min \leq v \leq V\max \end{cases} \quad (5)$$

For decreasing voltage one can model as a linear trend:

$$L_{CFL}(v) = A \times v + B \quad (6)$$

where, A and B are appropriate constant values.

TABLE IV

Lighting DUTs Voltage Range

| Curve/ DUTs | Nominal Voltage for AC supply [V] | Min [%] | Max [%] |
|---|---|---|---|
| CBEMA | 120 | 87 | 106 |
| ITIC | 120 | 90 | 110 |
| SEMI | 100 % | 90 | - |
| IEC Class 3 | 230 | 90 | - |
| EMerge A (DC) | 380 | 96 | 110 |
| Halogen Philips | 230 | 91 | 113 |
| Halogen Start | 230 | 91 | 113 |
| CFL Philips | 230 | 87 | 134 |
| CFL Osram | 230 | 70 | 130 |
| LED Philips | 230 | 104 | 147 |
| Lighting DUT limits | 230 | 91 | 115 |

The constants A, B, C, Vmin and Vmax have to be defined by a standard or be set depending on the load type. LED bulb has the same model as the CFL bulbs with different values for Vmin and Vmax. This type of load has the biggest hysteresis. Moreover, the internal electronics of LED bulbs have a range in which even though they start lighting the power is not sufficient to ensure steady-state operation and therefore they are assigned to an intermittent mode of operation.

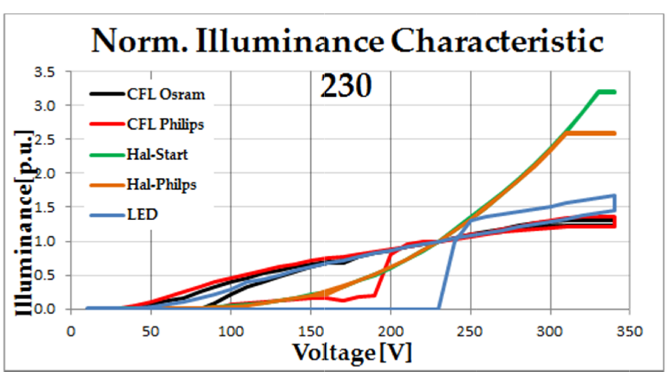


Figure 4. Illuminance Characteristics of Lighting DUTs normalized to 230 V value

Halogen bulb supply P(V) characteristic exhibits nohysteresis; the increasing and decreasing curve have the same trend line. The power and illuminance function model is an equation of second order.:

$$P_{HAL}(v) = A \times v^2 + B \times v + C \quad (7)$$

$$L_{HAL}(v) = A \times v^2 + B \times v + C \quad (8)$$

*3) All DUTs comparison*

From Tables III and IV a voltage range in which all DUTs operates is created. The upper limit is 115% and the lower is 91.3 % of the nominal voltage (230 V).

## *D. Conclusions*

A conclusion is flexibility of these devices/loads, because they could operate supplied by either a DC or AC source of energy.

The lighting DUTs voltage range is lower than not-lighting DUTs, but the limits of operation for the lightings are defined by the authors and not by a standard. Therefore, the results are highly dependant on the adopted definition of "acceptable operation of appliances."

# IV. POWER FLOW IN LV DCMGS

Compared to the traditional power flow (PF) models, for DC microgrids it is impractical to take any of the source buses as slack bus due to the fact that there are a small number of controllable generating units. The scope of the slack bus in the large power systems is to compensate whatever amount of real power imbalance may appear. Another difference with the AC microgrids, when trying to apply the traditional way of modeling of the PF analysis, is that it doesn't take the droop control parameters into consideration. However, droop coefficients proved to have decisive effects on the steady state characteristic of the system [13].

For a comprehensive, yet brief presentation of the PF formation for DC microgrids under droop control, a simple example is used here, as it is presented in Figure 5.

The known parameters in the PF formulation for DC MGs under droop control are: the impedances of the lines connecting the busses, and an estimation of the load demand at the load buses. This estimation is usually given by an upper layer management system, called the economic dispatch of the microgrid. The unknown variables, those that will be determined by solving the power flow equations, are the voltage magnitudes at each bus and the injected power at the generating buses.

The mathematical model of the power flow under droop is as follows:

$$I_i = \sum_{\substack{i=1 \\ i \neq j}}^{N} Y_{ij}(V_i - V_j) \quad (9)$$

$$P_i = V_i * I_i \quad (10)$$

$$\frac{P_i}{V_i} = \sum_{\substack{i=1 \\ i \neq j}}^{N} Y_{ij}(V_i - V_j) \quad (11)$$

$$\sum_{i=1}^{NS} P_{source,i} = \sum_{j=1}^{NL} P_{load,j} - P_{loss} \quad (12)$$

where, $I_i$ and $P_i$ are the current and power, respectively, injected ($P_{source,i}$) or withdrawn ($P_{load,j}$) from bus *i*; $Y_{ij} = 1/Z_{ij}$ is the admittance of the line defined by nodes *i* and *j;* $V_i$ and $V_j$ are the voltage magnitudes corresponding to bus *i* and bus *j*, respectively; *NS* and *NP* are the number of sources and respectively loads in the DC microgrid; and $P_{loss}$is the amount of power losses in the distribution network of the microgrid.

Equation (9) is the Kirchhoff current law applied to each node/bus *i*. Equation (10) describes the relationship between voltage and currents in a DC bus, and equation (11) was derived from (9) and (10). Equation (10) is the power balance for the whole system at an instance of time between consecutive PF loops. Besides (9) to (11), the source buses must also respect the droop equation (1).

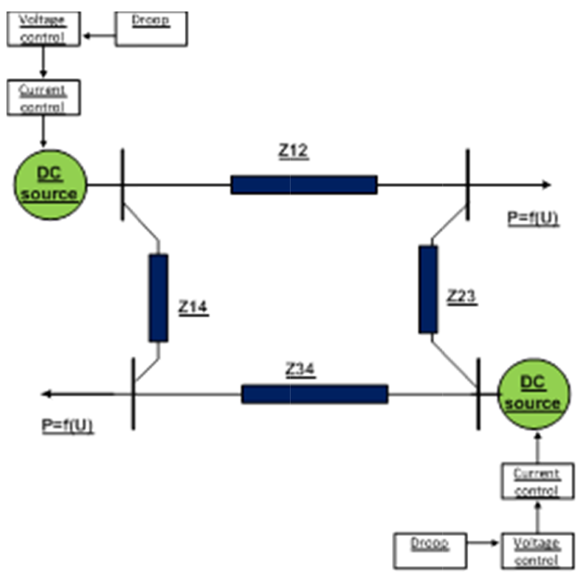


Figure 5. DC microgrid under droop control power flow

## V. EVALUATION OF RESULTS

A MATLAB/Simulink model was developed in discrete-time according to Figure 5. The details of the system are given in [15]. For comparison reasons we have kept the same values for the rated power of the loads. Note however, that the rated power for the loads are just the reference values, while in our implementation the actual power withdrawn at the specific bus was determined following a linear summation of non-linear characteristic of the loads, experimentally determined such that to reach the same power level. The voltage comparison of the voltage profiles of the buses, when considering realistic load models and the constant power load models is presented in Table V. The same droop coefficients as in [15] were kept constant for both situations. As it can be seen the voltage drop in the busses is much higher in the case of non-linear/non-constant power loads if no corrections are applied to the droop coefficients. In Table V, last column are given the corrected voltage profiles when droop coefficients were adjusted according to the load models experimentally derived.

TABLE V

| # bus | Power flow results for fixed droop coefficients calculated for CPL models | | Power flow results for adjusted droop coefficients to the actual load models | |
|---|---|---|---|---|
| | Voltage magnitude (p.u) | Power [W] | Voltage magnitude (p.u) | Power [W] |
| 1 | 0.872 | 826.42 | 0.9769 | 817.23 |
| 2 | 0.863 | 466.25* | 0.9742 | 466.25* |
| 3 | 0.855 | 337.15 | 0.9735 | 349.72 |
| 4 | 0.856 | 697.5* | 0.9750 | 697.5* |

Note: * is for given/known values in the PF model

## VI. CONCLUSIONS

This work proposed a generalized formulation of the power flow for DC microgrids operating under droop control power sharing. It was proven that, when considering only CPL models to calculate the droop coefficients in the power flow model, significant deviations from the calculated values to the measurements could take place. The paper experimentally evaluates for set of expected loads within office and residential buildings micro or nanogrids. These derived V-I characteristics were then used to accurately determine the droop coefficients in the proposed power flow model.

## ACKNOWLEDGMENT


This work has received funding from the European Union's Horizon 2020 R&I Programme under the Marie Sklodowska-Curie grant agreement No 708844.


## REFERENCES


[1] S. Chowdhury and P. Crossley, Microgrids and active distribution networks: The Institution of Engineering and Technology, 2009.

[2] P. Chiradeja and R. Ramakumar, "An approach to quantify the technical benefits of distributed generation," IEEE Transactions on Energy Conversion, vol. 19, no. 4, pp. 764-773, Dec. 2004.

[3] L. F. Ochoa, A. Padilha-Feltrin, and G. P. Harrison, "Evaluating Distributed Time-Varying Generation Through a Multiobjective Index," IEEE Transactions on Power Delivery, vol. 23, no. 2, pp. 1132-1138, Apr. 2008.

[4] N. Hatziargyriou, MicroGrids: Wiley-IEEE Press, 2014.

[5] N. Hatziargyriou. "Microgrids : architectures and control," http://search.ebscohost.com/login.aspx?direct=true&scope=site&db=nlebk&db=nlabk&AN=673177.

[6] M. Asprou and E. Kyriakides, "Enhancement of hybrid state estimation using pseudo flow measurements," IEEE Power and Energy Society General Meeting, Detroit, USA, pp. 1-7, 24-29 Jul. 2011.

[7] J. Rajagopalan, K. Xing, Y. Guo, F. C. Lee, and B. Manners, "Modeling and dynamic analysis of paralleled DC/DC converters with master-slave current sharing control," Conference Proceedings of Applied Power Electronics Conference and Exposition -APEC, pp. 678-684 vol.2, 3-7 Mar 1996.

[8] Q. Weihong and L. Zhixiang, "Practical design considerations of current sharing control for parallel VRM applications," Proceedings of the IEEE Conference on Applied Power Electronics - APEC, pp. 281-286, 6-10 Mar. 2005.

[9] J. M. Guerrero, J. C. Vasquez, J. Matas, L. G. d. Vicuna, and M. Castilla, “Hierarchical Control of Droop-Controlled AC and DC Microgrids: A General Approach Toward Standardization,” IEEE Transactions on Industrial Electronics, vol. 58, no. 1, pp. 158-172, 2011.

[10] N. L. Diaz, T. Dragicevic, J. C. Vasquez, and J. M. Guerrero, “Intelligent Distributed Generation and Storage Units for DC Microgrids: A New Concept on Cooperative Control Without Communications Beyond Droop Control,” IEEE Transactions on Smart Grid, vol. 5, no. 5, pp. 2476-2485, May 2014.

[11] T. Dragičević, X. Lu, J. C. Vasquez, and J. M. Guerrero, “DC Microgrids-Part I: A Review of Control Strategies and Stabilization Techniques,” IEEE Transactions on Power Electronics, vol. 31, no. 7, pp. 4876-4891, July 2016.

[12] Q. Shafiee, T. Dragicevic, J. C. Vasquez, and J. M. Guerrero, “Hierarchical Control for Multiple DC-Microgrids Clusters,” IEEE Transactions on Energy Conversion, vol. 29, no. 4, pp. 922-933, Apr. 2014.

[13] C. Li, S. K. Chaudhary, M. Savaghebi, J. C. Vasquez, and J. M. Guerrero, “Power Flow Analysis for Low-voltage AC and DC Microgrids Considering Droop Control and Virtual Impedance,” IEEE Transactions on Smart Grid, vol. PP, no. 99, pp. 1-11, Mar. 2016.

[14] J. Zhao and F. Dorfler, “Distributed control and optimization in DC microgrids,” Automatica, vol. 61, no. C, pp. 18-26, Nov. 2015.

[15] L. Chendan, S. K. Chaudhary, T. Dragicevic, J. C. Vasquez, and J. M. Guerrero, "Power flow analysis for DC voltage droop controlled DC microgrids," Proceedings of the IEEE 11th International Multi-Conference on Systems, Signals & Devices -SSD14, Barcelon, Spain, pp. 1-5, 11-14 Feb. 2014.

[16] L. Mackay, L. Ramirez-Elizondo, and P. Bauer, "DC ready devices - Is redimensioning of the rectification components necessary?," Proceedings of the 16th International Conference on Mechatronics, Brno, Czech Republic, pp. 1-5, 3-5 Dec. 2014.

[17] H. Tamaki, "Nushima Project: An Experimental Study on a Self-Sustainable Decentralized Energy System for an Isolated Island ", Microgrids-Symposium, Aalborg, pp. 1-14, 27-28 Aug. 2015.

[18] T. F. Wu, C. H. Chang, L. C. Lin, G. R. Yu, and Y. R. Chang, “DC-Bus Voltage Control With a Three-Phase Bidirectional Inverter for DC Distribution Systems,” IEEE Transactions on Power Electronics, vol. 28, no. 4, pp. 1890-1899, Apr. 2013.

[19] H. Kakigano, M. Nomura, and T. Ise, "Loss evaluation of DC distribution for residential houses compared with AC system," International Power Electronics Conference (IPEC), pp. 480-486, 21-24 June 2010.

[20] H. Kakigano, Y. Miura, and T. Ise, “Low-Voltage Bipolar-Type DC Microgrid for Super High Quality Distribution,” IEEE Transactions on Power Electronics, vol. 25, no. 12, pp. 3066-3075, Dec. 2010.

[21] "CBEMA curve – the power acceptability curve for computer business equipment," Technical Note, Power Quality in Electrical Systems, 2011, [Available online:] www.powerqualityworld.com/2011/04/cbema-curvepower-quality-standard.html.

[22] "SEMI F47: Specification for semiconductor processing equipment voltage sag immunity," Power Quality World, 2011, [Available online:] http://www.powerqualityworld.com/2011/04/semif47-semiconductor-voltage-sag.html.

[23] "Emerge alliance occupied space standard version 1.1," EMerge-Alliance, 2016 [Available online:] www.emergealliance.org/Standards/OccupiedSpace/RequestStandard.aspx.

[24] "Gleichstrom im Niederspannungsbereich, version 1," DEUTSCHE NORMUNGS-ROADMAP (in German) Feb. 2016.